A New Methodology to Investigate Fracture Toughness of Freestanding MEMS and Advanced Materials in Thin Film Form

Horacio D. Espinosa and Bei Peng

***Abstract*—This paper presents a novel membrane deflection fracture experiment (MDFE) to investigate the fracture toughness of microelectromechanical systems (MEMS) and other advanced materials in thin film form. It involves the stretching of freestanding thin-film membranes, in a fixed-fixed configuration, containing preexisting cracks. The fracture behavior of ultrananocrystalline diamond (UNCD), a material developed at Argonne National Laboratory, is investigated to illustrate the methodology. When the fracture initiates from sharp cracks, produced by indentation, the fracture toughness was found to be 4.5 ± 0.25 MP $\mathrm{m}^{1/2}$. When the fracture initiates from blunt notches with radii about 100 nm, machined by focused ion beam (FIB), the mean value of the apparent fracture toughness was found to be 6.9 MPa $\mathrm{m}^{1/2}$. Comparison of these two values, using the model proposed by Drory *et al.* [9], provides a correction factor of two-thirds, which corresponds to a mean value of $\rho/2x = 1/2$. [1083]**

***Index Terms*—Fracture toughness, microelectromechanical systems (MEMS), thin films, ultrananocrystalline diamond.**

I. Introduction

SIGNIFICANT research has been conducted on the design, modeling, and manufacturing of microelectromechanical systems (MEMS). However, long-term durability of various MEMS devices, which requires a fundamental understanding of microstructure-*fracture toughness* relationship, is just now been fully addressed in a systematic fashion. The fracture toughness K_{IC} provides an assessment of the resistance a material possesses to crack growth from a preexisting defect [1], [2]. K_{IC} depends only on microstructural factors and not on the specimen geometry, boundary conditions, and loading. Consequently, the best way to compare structures of different geometries is on the basis of their respective stress intensity levels.

To measure the fracture toughness K_{IC} at the scale of MEMS one needs experimental setups that either integrate the specimen to the loading device or that the specimen can be easily gripped and loaded by external actuators. These actuators need to be capable of providing sufficient force to ensure crack propagation.

Manuscript received June 26, 2003; revised May 24, 2004. This work was supported in part by the National Science Foundation by Career Award CMS-9624364, GOALI Award CMS-0120866/001, and by the Nanoscale Science and Engineering Initiative of the National Science Foundation by NSF Award EEC-0118025 and the DOE Office of Science under Contract N00014-97-1-0550. Subject Editor S. M. Spearing.

The authors are with the Department of Mechanical Engineering, Northwestern University, Evanston, IL 60208 USA (e-mail: espinosa@northwestern.edu).

Digital Object Identifier 10.1109/JMEMS.2004.839013

Furthermore, a technique able to produce atomically sharp preexisting cracks must be employed in the testing protocol. Concerning this feature, an indentation technique was successfully developed by Keller [3] to produce sharp cracks in micromachined MEMS specimens although no fracture results were reported. Using this technique, on-chip fracture mechanics studies were pioneered by Kahn *et al.* [4], [5], and Ballarini *et al.* [6]. By contrast, Sharpe *et al.* [7], and Tsuchiya *et al.* [8] performed tests on specimens containing notches, while Chasiotis and Knauss [9], [10] investigated *fracture strength* in perforated specimens. Fracture strength of polysilicon at stress concentrations was also recently investigated by Bagdhan *et al.* [11].

Kahn *et al.* [4], [5] and Ballarini *et al.* [6] reported the first on-chip fracture tests on polysilicon. The specimens were integrated with microfabricated electrostatic comb-drive actuators and loaded by applying a dc voltage. Displacements were measured by employing optical microscopy with an accuracy of $\sim 0.3\ \mu\mathrm{m}$. The measured fracture toughness of polysilicon exhibited a mean value of 1.1 $\mathrm{MPa\ m}^{1/2}$, which was found to be independent of polysilicon microstructure. The advantage of this technique is that the entire fracture experiment is performed at the chip level, thus, eliminating the difficulties associated with attaching the specimens to external loading sources. Sharpe *et al.* [7] and Tsuchiya *et al.* [8] employed microfabricated polysilicon specimens containing notches, which were loaded by external actuators. They reported a critical stress intensity factor K_{IC} of 1.4 and 1.9 to 4.5 $\mathrm{MPa\,m}^{1/2}$, respectively. These high values of K_{IC} are associated with the finite radii (1.0 and 0.23 $\mu\mathrm{m}$, respectively) of the notches and thus they do not represent the true fracture toughness of the material.

In the past, three techniques were used to produce preexisting defects in polysilicon thin film specimens. Indentation induced (1) and fatigue induced (2) cracked specimens were investigated by Kahn *et al.* [4] and Ballarini *et al.* [6]; while microfrabricated specimens containing notches with finite radii (3) were tested by Sharpe *et al.* [7], and Tsuchiya *et al.* [8]. As various techniques were used to deposit the polysilicon films and manufacture the defects, results on K_{IC} varying from 1.1 to 4.5 $\mathrm{MPa\,m}^{1/2}$ were reported. The scattering in the data can be attributed to the fact that a notch results in *stress intensification* rather than a singular field. Drory *et al.* [12] investigated the failure of microcrystalline diamond and proposed a model to estimate K_{IC} from specimens containing notches. However, the toughness identified with this procedure is only a lower bound estimate.

In this paper, a new membrane deflection fracture experiment (MDFE) is used to investigate fracture toughness. The

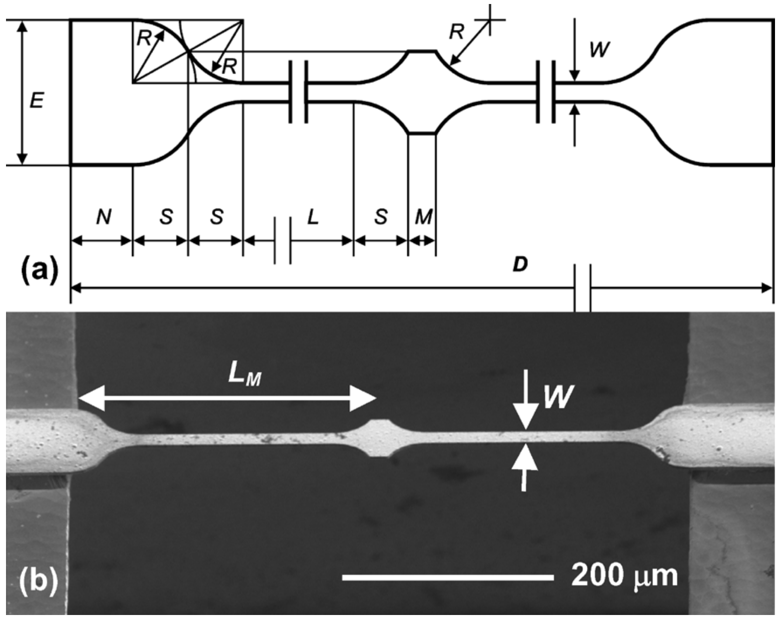

Fig. 1. (a) Schematic of membrane geometry indicating the different parameters used to define specimen dimensions; here $\mathrm{E} = 100\ \mu\mathrm{m}$, $\mathrm{R} = 40\ \mu\mathrm{m}$, $\mathrm{W} = 20\ \mu\mathrm{m}$, $\mathrm{N} = 20\ \mu\mathrm{m}$, $\mathrm{L} = 200\ \mu\mathrm{m}$, $\mathrm{S} = 34.64\ \mu\mathrm{m}$, $\mathrm{M} = 20\ \mu\mathrm{m}$, $\mathrm{D} = 667.84\ \mu\mathrm{m}$. (b) Scanning electron microscopy (SEM) image of UNCD membranes showing characteristic dimensions. L_M is half the membrane span, and W is the membrane width.

technique offers certain advantages such as the loading procedure is straightforward and accomplished in a highly sensitive manner. The simplicity of sample microfabrication and ease of handling make this technique particularly suitable for routine on-chip screening of material properties. As an example, the toughness of ultrananocrystalline diamond (UNCD) thin films is investigated. UNCD is a material developed at Argonne National Laboratory with unique properties particularly suitable to the development of novel MEMS/NEMS [13], [14]. The material in its undoped form has a Young's Modulus of 960 GPa and a strength of 4.2 GPa, at 63% failure probability, according to Weibull theory [14]. The high stiffness and brittleness of UNCD make the measurement of its fracture toughness particularly challenging. However, the MDFE here reported is capable of providing sufficient force and elongation to ensure crack propagation. Two types of specimens are tested and compared: blunt-notched specimens with notch tip radii of $\sim 100\ \mathrm{nm}$ and specimens containing sharp cracks. The theory by Drory *et al.* [12] is used to account for the effect of notch radius and the ambiguity in the dimensionless parameter $\rho/2x$ is eliminated by matching measurements performed on notched specimens with radius of curvature ρ and atomically sharp cracks. The results are discussed in the context of MEMS applications.

II. Experimental Methodology

A. Specimen Design and Microfabrication

The specimen geometry utilized in this study resembles the typical dog-bone tensile specimen but with an area of additional width in the specimen center designed to prevent failure at the point of application of a line load [see Fig. 1(a)] [15]. The suspended membranes are fixed to the wafer at both ends such that they span a bottom view window [Fig. 1(b)]. In the areas where the membrane is attached to the wafer and in the central area the width is varied in such a fashion to minimize boundary-bending effects and prevent bending failure at these locations. These effects are also minimized through large specimen gauge lengths. Thus, a load applied in the center of the span results in direct stretching of the membrane in the two areas of constant width in the same manner as in a direct tension test. In this study, membranes with nominal dimensions of length $\mathrm{L}_M = 334\ \mu\mathrm{m}$, width $\mathrm{W} = 20\ \mu\mathrm{m}$, and thickness $\mathrm{t} = 0.8\ \mu\mathrm{m}$ were tested [see Fig. 1(b)].

The film was grown directly onto a Si substrate using a microwave plasma chemical vapor deposition technique based on a $\mathrm{CH_4}$/Ar chemistry [16]. The specimens were microfabricated using standard processes. The following is a summary of the steps used in their microfabrication (see Fig. 2).

- Step 1) Growth of UNCD on silicon substrate ($\sim 1.0\ \mu\mathrm{m}$). Deposition of a 300 nm Al film by e-beam evaporation. Al is used as mask material due to its resistance to oxygen reactive ion etching (RIE), which is employed to etch UNCD. Deposition and patterning of $\mathrm{Si_3N_4}$ film ($\sim 0.5\ \mu\mathrm{m}$ thick) on the other side of the silicon wafer. $\mathrm{Si_3N_4}$ is employed as a mask during KOH etching of $\langle 100\rangle$ silicon.
- Step 2) Photoresist, S1805, spin coating, prebaking, and exposure with mask aligner (Karl Suss MA6). Resist development and postbaking. Wet chemical etching of Al.
- Step 3) KOH etching from backside, 9 h (KOH 30% at $80\,^\circ\mathrm{C}$). The UNCD film is used as etching stop layer to define windows under the membranes.
- Step 4) $\mathrm{O_2}$-RIE, 50 mtorr, 200 W, various times, until the exposed UNCD is etched away. During the RIE etching, the photoresist is also removed. Removal of Al masks using wet etching.

Two techniques were used to produce the preexisting defects resulting in two types of specimens. The first one used focused

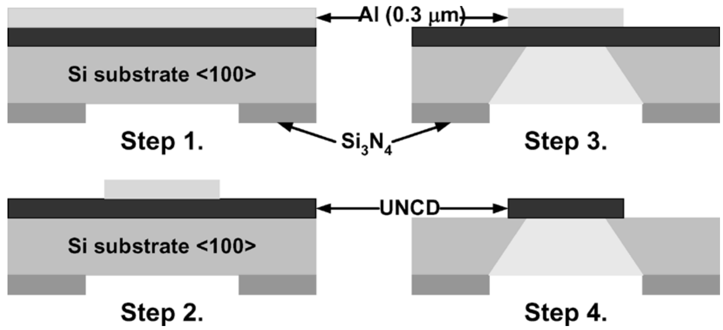

Fig. 2. Cross-sectional view of the microfabrication steps to obtain freestanding UNCD membranes.

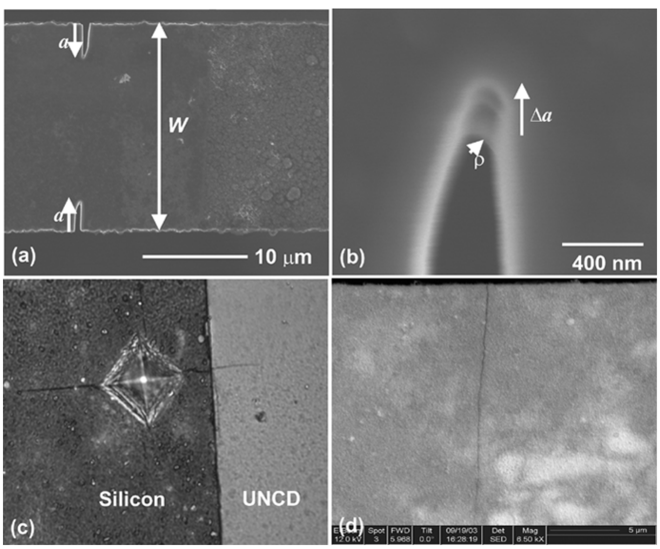

Fig. 3. (a) SEM micrograph of a prenotched specimen milled by FIB. (b) Magnified view of the notch tip region showing a blunt tip with a radius of approximately 100 nm and a length uncertainty Δa due to milling errors. (c) Optical image showing a sharp crack induced from an indent on the silicon substrate before specimen release. (d) SEM micrograph of the crack after specimen release. Crack length was measure from SEM images.

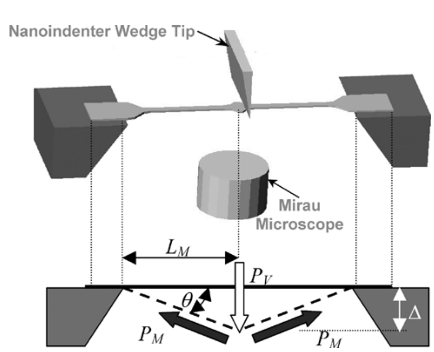

Fig. 4. A schematic drawing of the MDFE setup. Parameters are defined in the text.

ion beam (FIB) micromilling with a beam current density of 15 $\mathrm{A/cm^2}$ and a beam diameter of 10 nm. Two notches with the same length were milled simultaneously. A symmetric edge-cracks configuration was obtained. The geometry of the specimen is shown in Fig. 3(a). Blunt notches with tip radii of $\sim$ 100 nm were produced [see Fig. 3(b)]. In this configuration, an *apparent* fracture toughness can be computed from the following [17]

$$K'_{IC} = \sigma_f \sqrt{\pi a} f\left(\frac{a}{W}\right) \tag{1}$$

$$f\left(\frac{a}{W}\right) = 1.12 + 0.43\left(\frac{a}{W}\right) - 4.78\left(\frac{a}{W}\right)^2 + 15.44\left(\frac{a}{W}\right)^3 \tag{2}$$

where σ_f is the failure stress, a is the length of the cracks, and W is the width of the gauge region as shown in Fig. 3(a).

The second technique achieved an atomically sharp crack by placing a Vickers indent (with a 200-g load) near the specimen prior to its release by KOH etching. Although the indent was placed on the silicon substrate [see Fig. 3(c)] the radial cracks, which initiated at the indent corners, propagated into the UNCD specimens. The length of the crack was measured using high resolution SEM, see Fig. 3(d). This technique for forming sharp cracks in micromachined MEMS specimens was first proposed by Keller [3], though no fracture results were reported. An edge-crack model was used to compute $\mathrm{K_I}$ for the second type of specimen. In this geometry, the function $f(a/W)$ is given by

$$f\left(\frac{a}{W}\right) = 1.12 - 0.23\left(\frac{a}{W}\right) + 10.55\left(\frac{a}{W}\right)^2 - 21.72\left(\frac{a}{W}\right)^3. \tag{3}$$

B. Methodology

The membrane deflection experiment (MDE) was used to achieve direct tensile stressing of the specimen until failure [15]. The procedure involves applying a line-load, with a nanoindenter, at the center of the spanning membrane. Simultaneously, an interferometer focused on the bottom side of the membrane records the deflection. The result is direct tension of the two gauge regions with load and deflection measured independently. A schematic of the membrane deflection experimental setup is shown in Fig. 4. It consists of a nanoindenter, to apply load to the center of the membrane from the top, and a Mirau microscope interferometer, positioned directly below the specimen, to independently measure deflection through the microfabricated silicon window.

The data directly obtained from the MDE must then be reduced to arrive at a stress history for the membrane. The load

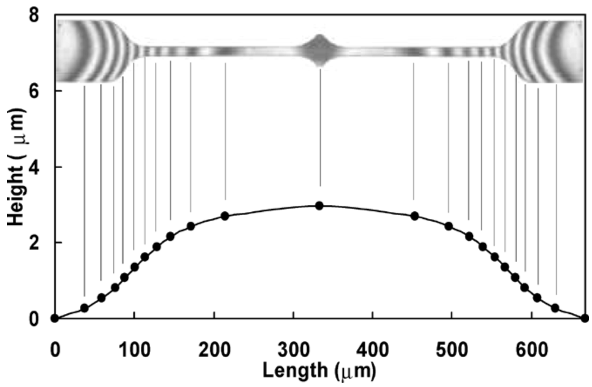

Fig. 5. Interferometric characterization of freestanding UNCD specimen. Out-of-plane bulging due to residual stresses is observed.

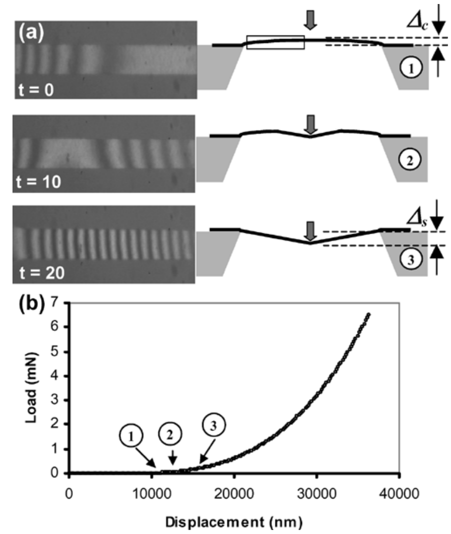

Fig. 6. (a) Schematic representations of the side-view of the MDFE test at three different time intervals. Δ_c is the vertical displacement at the middle of the span and Δ_s is the deflection at which uniform straining of the membrane begins. (b) Representation of the three states shown in (a) on the load-displacement curve.

in the plane of the membrane is found as a component of the vertical nanoindenter load by the following

$$\tan\theta = \frac{\Delta}{L_M} \text{ and } P_M = \frac{P_V}{2\sin\theta} \tag{4}$$

where (from Fig. 4) θ is the angle of deflection, Δ is the displacement, L_M is the membrane half-length, P_M is the load in the plane of the membrane, and P_V is the load measured by the nanoindenter. Once P_M is obtained, the nominal stress $\sigma(t)$ can be computed from

$$\sigma(t) = \frac{P_M}{A} \tag{5}$$

where A is the cross-sectional area of the membrane in the gauge region. The calculation of strain, away from the defects regions, was performed following the procedure given in [14], [15].

An important aspect of the UNCD specimens was that each membrane bowed upward as processed, i.e., out of the wafer plane. This is believed to result from the difference in thermal expansion coefficients, between the film and Si wafer, such that cooling down from the deposition temperature, approximately 800 °C, resulted in the Si shrinking more than the UNCD film. Fig. 5 shows a typical interferometric image and the generated x-z profile. This profile was obtained from the knowledge that the vertical distance between two dark fringes is half of the wavelength of the monochromatic green light used in the imaging ($\lambda/2 = 270$ nm).

Fig. 6(a) shows a series of optical images taken at different time intervals during a typical UNCD membrane deflection fracture experiment. A schematic side view of the membrane is shown to the right of each frame. The first frame shows the state of the membrane just before contact is made. The height above the plane of the wafer Δc is determined as illustrated in Fig. 5. The successive frame shows contact and deflection of the membrane. The process occurs in a smooth manner as seen by the inflection point, denoted by the arrows, moving toward the fixed end of the membrane. The final frame shows the deflection where uniform stretching of the membrane begins. This state can be determined by computing the downward deflection Δs such that the membrane becomes straight and uniform straining of the material begins. Fig. 6(b) shows different time intervals during a typical test with corresponding points on the load-deflection signature. Uniform stretching of the membrane begins at point 3. Note that a nonzero load is needed to achieve this configuration.

III. Results and Discussion

Fig. 7 shows a typical strain-stress signature of a notched UNCD specimen. Both stress and strain are computed away from the notch, i.e., where a homogeneous deformation field develops. The far-field stress is used to compute the material toughness by means of (1). The slope of the plot represents the elastic modulus (960 GPa). Failure occurs at a maximum stress of 2.3 GPa in a perfectly brittle fashion.

Fifteen specimens with the FIB-machined notches were tested under the same condition except that the notch length a was varied from 1 to 5 microns. The ratio of the notch length and specimen width a/W is in the range of 0.05–0.25. The dimensions a and W were measured using SEM. The *apparent* fracture toughness of the blunt notched specimens was then computed using (1) and (2).

Values of $K'_{IC} = 6.9 \pm 0.4$ MPa m$^{1/2}$ were obtained (Table I). From Table I it is clear that the apparent fracture toughness is independent of the crack length. This suggests that only the region of the material immediately in front of the crack like defect affects the fracture toughness. In all tested specimens failure occurred from the notch tip. This is illustrated in Fig. 8(a) in which an SEM image of four tested membranes is shown. All the specimens broke at the place where the symmetrically fabricated notches were positioned. Fig. 8(b) is a magnified image of a failed region showing that the failure propagated from notch tip to notch tip. The fracture surface exhibits a roughness consistent with the material grain size and microstructure. It is expected that the crack propagation speed would be very high because UNCD has a large elastic modulus and a low density. Fig. 8(c) and (d) shows a magnified

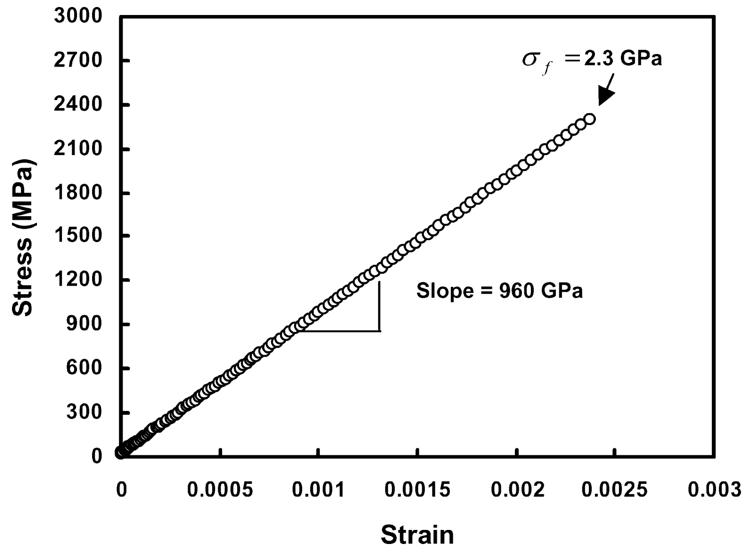

Fig. 7. Strain-stress curve of a typical fracture test. In this case, the fracture stress $\sigma_f = 2.3$ GPa corresponds to a specimen with a notch length $a = 2.2$ μm.

TABLE I
FRACTURE TOUGHNESS MEASUREMENT ON 15 UNCD SPECIMENS WITH NOTCHES

Sample Number	a (μm)	$\sigma_f^{(exp)}$ (GPa)	K'_{IC} (Eq. 1, 2) [MPa m$^{1/2}$]	K_{IC} with blunt notch correction [MPa m$^{1/2}$]
1	1.0	3.23	6.6	4.4
2	1.7	2.69	7.1	4.7
3	1.7	2.46	6.5	4.3
4	2.0	2.27	6.5	4.3
5	2.1	2.41	7.0	4.7
6	2.2	2.28	6.9	4.6
7	2.3	2.19	6.8	4.5
8	2.4	2.14	6.7	4.5
9	2.7	2.08	7.0	4.7
10	3.5	1.78	6.8	4.5
11	3.5	1.88	7.1	4.7
12	3.7	1.68	6.6	4.4
13	4.0	1.67	6.9	4.6
14	4.1	1.73	7.2	4.8
15	4.9	1.53	7.3	4.9
Mean values	---	---	6.9±0.25	4.6±0.18

view of the fracture plane at both sides of the specimen. The prenotch and the fracture regions can be easily identified from the surface roughness features.

It is important to note that in the computation of the K'_{IC} values, the notch was replaced by an apparent crack. Hence, corrections must be made because the effect of the blunt notch is to reduce the stress intensity relative to that ahead of a sharp crack. If this effect is not considered, resulting fracture toughness values become erroneously high.

From the above discussion, the deviation from the sharp crack assumption, (1), needs to be corrected. For a blunt tip the asymptotic stress field is given by [18]

$$\sigma_y(x) = \frac{K}{\sqrt{2\pi x}}\left(1 + \frac{\rho}{2x}\right) \tag{6}$$

where the origin of the reference system is in the middle between the tip and the center of the circular blunt notch, so that $x > \rho/2$. Comparing this stress field with the corresponding one for a sharp crack ($\rho \to 0$), Drory *et al.* [12], proposed the following correction

$$K_{IC} = \frac{K'_{IC}}{1 + \frac{\rho}{2x}} \tag{7}$$

in which K'_{IC} is the measured *apparent* fracture toughness from a blunt notch, ρ is the notch root radius, and x is a radial distance. Since the value of $\rho/2x$ is not determined, Drory *et al.* [12] assume $\rho/2x$ to be 1 providing a lower bound for K_{IC}. Consequently, they propose a 50% reduction on the measured fracture toughness to take into account the presence of the blunt tip [12]. By measuring the toughness in a specimen containing an indentation induced crack, an assessment of this correction was made. As shown in Fig. 3(d), cracks produced by indentation can be assumed atomically sharp, therefore, (1) and (3) can be employed to compute the fracture toughness of the material. Several experiments performed on specimens containing these cracks, resulted in a toughness $K_{IC} = 4.5$ MPa $\cdot$ m$^{1/2}$ (see

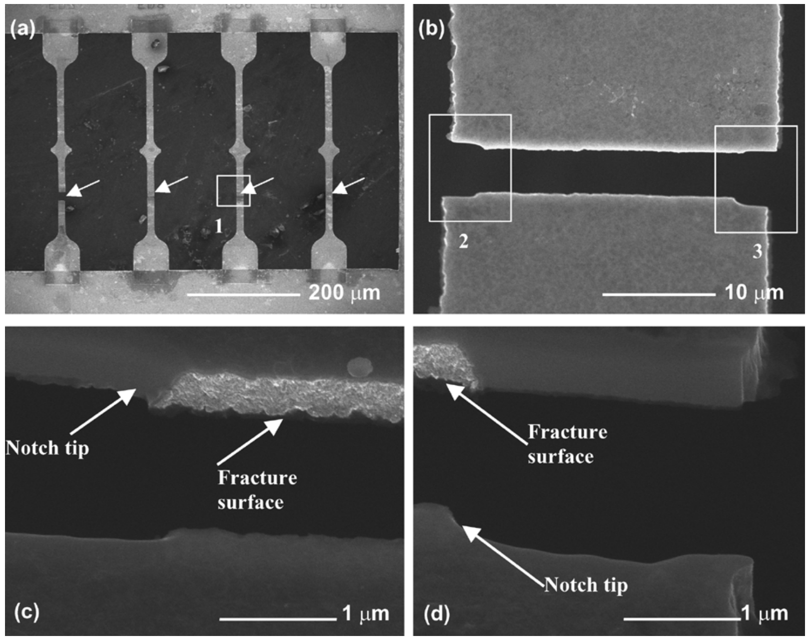

Fig. 8. SEM image showing four MDFE specimens after testing. The images (a) illustrate that failure indeed occurs in precracked regions. (b) An enlarged top-view of the fracture region in window 1. (c) and (d) Fracture surface near the notch tips illustrating features of the propagating crack.

TABLE II
FRACTURE TOUGHNESS MEASURED FROM SHARP CRACKS

a (μm)	W (μm)	$\sigma_f^{(exp)}$ [GPa]	K_{IC} (Eq. 3) [MPa m$^{1/2}$]
2.1	18.1	1.35	4.1
3.9	18.2	0.95	4.4
5.8	18.0	0.80	4.8
6.6	18.2	0.71	4.5
8.2	18.1	0.75	4.4

Average K_{IC} = 4.5 MPa m$^{1/2}$; Standard Deviation = 0.25 MPa m$^{1/2}$

TABLE III
FRACTURE TOUGHNESS OF MEMS MATERIALS

Material	K_{IC} (Mpa m$^{1/2}$)
Si <111>	0.83-0.95 [19]
Glass	~1 [2]
Polysilicon	1.1-1.9 [4-8]
Al_2O_3	3-4 [2]
SiC	3.3 [20]
Si_3N_4	4.1 [21]
Microcrystalline Diamond	5.6 [12]
UNCD	4.6 [This work]

Table II). Therefore, for an average K'_{IC} of 6.9 $\mathrm{MPa}\cdot\mathrm{m}^{1/2}$, we find that $\rho/2x$ should be 0.53, which coincides with the mean value of $\rho/2x$, which is 1/2. Consequently, we propose to employ a correction factor in (7) of two-thirds. The corrected toughness values are shown in Table I.

The results obtained in this work shows that the tested UNCD exhibits a fracture toughness larger than that of other MEMS materials such as Si, Polysilicon, SiC, Al_2O_3, and Si_3N_4, but slighter smaller than that of Microcrystalline Diamond (Table III).

IV. CONCLUSION

A new methodology for the fracture toughness measurement of thin films and MEMS materials was presented. The MDFE is a simple and robust method to investigate fracture toughness of MEMS materials in mode I. The technique can be used to interrogate both cracks obtained by indentation and notches microfabricated by FIB or other techniques as long as needed corrections are performed, see also Pugno *et al.* [22]. In this investigation, we obtained notches about 100 nm in radius. It is possible that the sharpness of the notch can be improved by using a more precise focused ion beam system or other milling parameters. Fracture toughness of UNCD thin films was consistently measured. A correction factor, to take into account the presence of the blunt tip, is also proposed. Results indicate that the fracture toughness of UNCD is independent of the crack length as expected from fracture mechanics theory. The high strength and toughness of UNCD films established in this paper and [14] indicates that the material is ideal for the development of novel MEMS/NEMS devices. In contrast to microcrystalline diamond, UNCD is much more conformal. Continuous films with a thickness as small as 50 nm can be obtained when a large number of nucleation sites are induced by ultrasonic seeding. Future work will focus on fracture measurements on different materials, including doped UNCD, to investigate the relationship between toughness and microstructures.

ACKNOWLEDGMENT

The authors thank O. Auciello, J. Carlisle, and D. Gruen for providing the UNCD films. The authors would like to acknowledge N. Moldovan for assistance in the microfabrication of the specimens and many insightful suggestions.

REFERENCES

[1] J. F. Knott, *Fundamentals of Fracture Mechanics*. London, U.K.: Butterworths, 1973.
[2] R. W. Hertzberg, *Deformation and Fracture Mechan. Eng. Mater.*, pp. 315–325, 1996.
[3] C. Keller, "Microfabricated high aspect ratio silicon flexures," in *MEMS Precision Instrum.*, El Cerrito, CA, 1998, pp. 185–202.
[4] H. Kahn, N. Tayebi, R. Ballarini, R. L. Mullen, and A. H. Heuer, "Fracture toughness of polysilicon MEMS devices," *J. Sens. Actuators*, vol. 82, pp. 274–280, 2000.
[5] H. Kahn, B. Ballarini, R. L. Mullen, and A. H. Heuer, "Electrostatically actuated failure of microfabricated polysilicon fracture mechanics specimens," *Royal Soc. London A*, vol. 455, pp. 3807–3823, 1999.
[6] R. Ballarini, R. L. Mullen, Y. Yin, H. Kahn, S. Stemmer, and A. H. Heuer, "The fracture toughness of polysilicon microdevices: A first report," *J. Mater. Res.*, vol. 12, pp. 915–922, 1997.
[7] W. N. Sharpe, B. Yuan, and R. L. Edwards, "Fracture tests of polysilicon film," in *MRS Symp. Proc.*, vol. 505, Boston, MA, Dec. 1–5, 1997, pp. 51–56.
[8] T. Tsuchiya, J. Sakata, and Y. Taga, "Tensile strength and fracture toughness of surface micromachined polycrystalline silicon thin films prepared under various conditions," in *MRS Symp. Proc.*, vol. 505, Boston, MA, Dec. 1–5, 1997, pp. 285–290.
[9] I. Chasiotis and W. G. Knauss, "The mechanical strength of polysilicon films: Part 1. The influence of frabrication governed surface conditions," *J. Mech. Phys. Solids*, vol. 51, pp. 1533–1550, 2003.
[10] ——, "The mechanical strength of polysilicon films: Part 2. Size effects associated with elliptical and circular perforations," *J. Mech. Phys. Solids*, vol. 51, pp. 1551–1572, 2003.
[11] J. Bagdahn and W. N. Sharpe, "Fracture strength of polysilicon at stress concentrations," *J. Electromech. Syst.*, vol. 12, pp. 302–312, 2003.
[12] M. D. Drory, R. H. Dauskardt, A. Kant, and R. O. Ritchie, "Fracture of synthetic diamond," *J. Appl. Phys.*, vol. 78, pp. 3083–3088, 1995.
[13] D. M. Gruen, "Nanocrystalline diamond films," *Ann. Rev. Mater. Sci.*, vol. 29, pp. 211–259, 1999.
[14] H. D. Espinosa, B. C. Prorok, B. Peng, K.-H. Kim, N. Moldovan, O. Auciello, J. A. Carlisle, D. M. Gruen, and D. C. Mancini, "Mechanical properties of ultrananocrystalline diamond thin films relevant to MEMS devices," *J. Experimental Mechan.*, vol. 43, no. 3, pp. 256–268, 2003.
[15] H. D. Espinosa, B. C. Prorok, and M. Fischer, "A methodology for determining mechanical properties of freestanding thin films and MEMS materials," *J. Mechan. Phys. Solids*, vol. 51, pp. 47–67, 2003.
[16] D. M. Gruen, S. Liu, A. R. Krauss, J. Luo, and X. Pan, "Fullerenes as precursors for diamond film growth without hydrogen or oxygen additions," *Appl. Phys. Lett.*, vol. 64, pp. 1502–1504, 1994.
[17] *Stress Intensity Factors Handbook*, Y. Murakami, Ed., Pergamon, Oxford, U.K., 1987.
[18] M. Creager and P. C. Paris, *Int. J. Fracture Mech.*, vol. 3, p. 247, 1967.
[19] F. Ericson, "Hardness and fracture toughness of semiconducting materials studied by indentation and erosion techniques," *Mater. Sci. Eng.*, vol. A 105/106, pp. 131–141, 1988.
[20] J. L. Henshall, D. J. Rowcliffe, and J. W. Edington, "Fracture toughness of sigle-crystal silicon carbide," *J. Amer. Ceram. Soc.*, vol. 60, pp. 373–375, 1977.
[21] D. Chakraborty, A. K. Mukhopadhyay, and J. Mukerji, "Influence of thermal quenching on surface fracture toughness and microhardness of Si_3N_4, SiAlON, and SiC," *Rev. Internationale Des Hautes Temper. et Des Refractaires*, vol. 22, pp. 105–113, 1985.
[22] N. Pugno, B. Peng, and H. D. Espinosa, "Predictions of strength in MEMS components with defects—A novel experimental-theoretical approach," *Int. J. Solids and Structures*, 2004, submitted for publication.

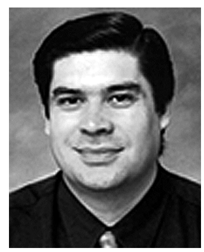

Horacio D. Espinosa received the degree in civil engineering from the Northeast National University, Argentina, in 1981, the M.Sc. degree in structural engineering from Politecnico di Milano, Italy, in 1987, and the M.Sc. and Ph.D. degrees, both in applied mathematics, from Brown University, in 1991 and 1992, respectively.

He then joined Purdue University and later, moved to Northwestern University in 2000. He is currently an Associate Professor with the Department of Mechanical Engineering, Northwestern University. His research interests are size scale plasticity and fracture of thin films and MEMS/NEMS materials, *in situ* electron and atomic probe microscopy testing of nanowires and CNTs, bioinspired design of materials, and the development of MEMS devices for massively parallel atomic probe writing with chemicals and biomolecules.

Prof. Espinosa is the recipient of two young investigator awards, NSF-Career and ONR-YIP, and a Junior Award from the American Academy of Mechanics (AAM). He is also Fellow of the American Society of Mechanical Engineers (ASME) and AAM. He is Editor of *Mechanics*, a publication of the AAM and Associate Editor of the journal *Experimental Mechanics*.

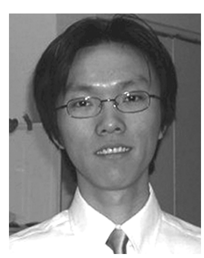

Bei Peng received the Bachelor's degree in mechanical engineering from the Beijing University of Aeronautics and Astronautics, China, in 1999 and the M.S. degree in mechanical engineering from Northwestern University in 2002. As a master's degree student, he was involved in investigating the elasticity, plasticity, and fracture of thin films relevant to MEMS devices.

He is currently pursuing the Ph.D. degree in mechanical engineering at Northwestern University. His research interests and activities include mechanical testing of thin film materials at micro- and nanoscale, MEMS design and fabrication, nanomanipulation of nanowires and CNTs, and mechanical testing at nano-scale, surface micromachining, contact mode AFM potentiometry, and nanomanipulation.